Fluorescent Silver Nanoclusters as Effective Probes for Highly Selective Detection of Mercury(II) at Parts-per-Billion Levels

Chuanxi Wang,[a] Lin Xu,[a] Yu Wang,[a] Dan Zhang,[a] Xiaodong Shi,*[b] Fengxia Dong,[a] Kui Yu,[c] Quan Lin,*[a] and Bai Yang[a]

Abstract: Facile preparation of water-soluble and fluorescent Ag nanoclusters (NCs) stabilized by glutathione at room temperature is described. Although the glutathione layer was introduced to prevent the silver nanoparticles from decomposition and increase their water solubility, this simple surface optimization resulted in surprisingly high efficiency of selective Hg^{2+} sensing, where the limit of detection (LOD) was as low as 10^{-10} M (0.02 ppb, 0.1 nM). This result revealed a simple and practical strategy for Hg^{2+} detection using fluorescent Ag NCs as sensor probe, with the lowest detecting limits reported to date.

Keywords: nanoclusters · fluorescent probes · mercury · selective detection · silver

Introduction

Metal nanoclusters (NCs) with discrete energy levels, bridging the "missing link" between atomic and nanoparticle behavior, show molecule-like electronic transitions within the conduction band and exhibit strong fluorescence.[1] Although among them silver NCs showed bright fluorescence in solution, there is an enduring challenge to prepare stable and water-soluble fluorescent Ag NCs under mild conditions.[2] Recently, various additives, such as DNA, oligonucleotides, proteins, polymers, and macromolecule hydrogels, have been employed in the synthesis of Ag NCs.[3] These additives provided a protecting layer on the surface of the Ag NCs to improve their stability and water solubility. However, these macromolecular templates resulted in the formation of Ag NCs with large hydrodynamic radii, which limited the scope of potential applications.[4] To reach the desired smaller size, frozen solution and zeolite were usually applied as the templates.[5] Again, the rather complicated synthetic procedure and constrained accessibility to the materials greatly limited application of the Ag NCs. Overall, simple, practical preparation methods for small Ag NCs from low-cost starting materials are highly desirable.

As is well known, the highly toxic mercuric ion (Hg^{2+}), which is in the 18-electronic configuration, has the capability to coordinate to mercaptan sulfur atoms in proteins, thus resulting in severe damage to the central nervous system.[6] In addition, the harm done by Hg^{2+} to the environment is another serious issue that we cannot afford to ignore.[7] Although various fluorescent probes for Hg^{2+} have been prepared, highly sensitive and selective detection of Hg^{2+} in water is essential.[8] To date, fluorescent gold NCs have been used as fluorescent probes for Hg^{2+}.[9] Concerning Ag NCs, protein-templated and oligonucleotide-stabilized Ag NCs have been used as fluorescent probes for Hg^{2+} as well.[10,3d] However, very few studies have reported fabrication of small-molecule-stabilized, especially small-biomolecule-stabilized luminescent Ag NCs as fluorescent probes.[4b] Herein, we report the successful synthesis of water-soluble and fluorescent Ag NCs from glutathione-templated hydrazine reduction. More importantly, these new Ag NCs exhibited extremely high selectivity toward Hg^{2+} over other cations (including Cd^{2+}, Zn^{2+}, Fe^{3+}, and Pb^{2+}), giving high sensitivity at 0.1 nM (0.02 ppb).

[a] Dr. C. Wang, L. Xu, Y. Wang, D. Zhang, F. Dong, Prof. Q. Lin, Prof. B. Yang
State Key Laboratory of Supramolecular Structure and Materials
College of Chemistry, Jilin University
Changchun, 130012 (P. R. China)
E-mail: linquan@jlu.edu.cn

[b] Prof. X. Shi
C. Eugene Bennett Department of Chemistry
West Virginia University
Morgantown, WV 26506 (USA)

[c] Prof. K. Yu
Steacie Institute for Molecular Sciences
NRC Canada
Ottawa, Ontario, K1 A0R6 (Canada)

Supporting information for this article is available on the WWW under http://dx.doi.org/10.1002/asia.201200033.

Results and Discussion

Our rationale was to investigate the possibility of using thiol small molecules as templates and protecting layers for the preparation of small and fluorescently active Ag NCs.[11] Driven by this hypothesis, glutathione (GSH) caught our immediate attention.[12] First, this small tripeptide possesses rich functional groups, including the free thiol, which can be used readily for metal nanoparticle surface modification.[13] The amide, carboxy, and free amine groups are all well-known binding handles for metal coordination, which can

help the coordination of selected metal cations right on the surface of the Ag NCs to achieve the effective metal sensing (which was demonstrated to be case in selective Hg^{2+} sensing; see below).[14] In addition, the hydrophilic nature of the peptide can greatly improve the solubility of the NCs in water, which is crucial for many biological and chemical operations. After screening various preparation conditions, a general protocol was developed.

As shown in Scheme 1, addition of $AgNO_3$ to aqueous GSH resulted in the formation of light yellow supramolecular hydrogel when the pH value of the solution reached 1.88. Then 1 M NaOH solution was added to the resulting hydrogel until the pH value was up to 6.45. A colorless transparent solution was obtained. Various reducing re-
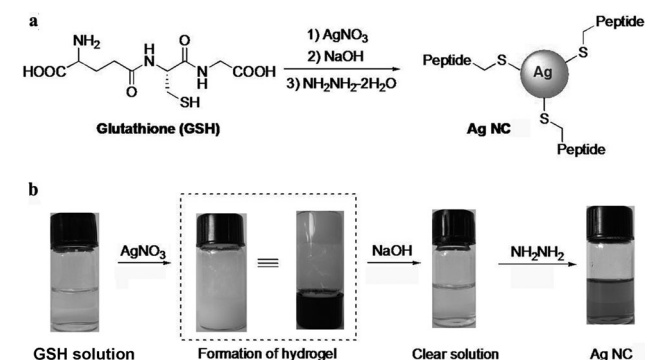
Scheme 1. Preparation of water-soluble and fluorescent Ag NCs.

agents were investigated for the formation of Ag NCs, and $NH_2NH_2 \cdot 2H_2O$ was identified as the optimal reductant. Hydrazine was injected slowly into the reaction mixture until the pH value of the solution was above 10. The resulting colorless solution was then left at room temperature for 11 h, giving the orange-yellow Ag NCs solution. The GSH-Ag NCs complexes were precipitated by the addition of isopropyl alcohol, collected through centrifugation at 8000 rpm, and then redispersed in water. The purification process was repeated three times at room temperature. The Ag NCs were readily dispersed in water, thus indicating their excellent water solubility.

This preparation procedure was simple and robust. The surface chemistry of resulting Ag NCs was characterized by FTIR spectroscopy and X-ray photo-

electron spectroscopy (XPS). The disappearance of the characteristic S−H stretching band at 2526 cm^{-1} in FTIR spectra after the formation of the NCs supported the proposed formation of Ag-GSH complexes through the Ag−S interactions (see the Supporting Information, Figure S1).[15] The detailed XPS spectra are provided in the Supporting Information, Figure S2. The peaks at 368.1 and 374.0 eV observed by XPS corresponded to Ag $3d_{5/2}$ and Ag $3d_{3/2}$, which indicated the formation of Ag^0 as expected after the reduction (see the Supporting Information, Figure S2a).[16] The peak at 161.9 eV was characteristic of S $2p_{3/2}$ (seen the Supporting Information, Figure S2b). There was no free thiol value in the range of 164 eV, which suggested that GSH-Ag metal thiolates were formed.[17] The result was consistent with the result of FTIR spectra. A new peak appeared at a binding energy of 287.8 eV, corresponding to C 1s of C−O and C=O (see the Supporting Information, Figure S2c).[18] The N 1s spectrum showed the peaks at binding energy values of 399.5 and 401.1 eV, indicating the presence of NH and NH_3^+, respectively (see the Supporting Information, Figure S2d). The peak at 531.1 eV corresponded to the binding energy of O 1s (see the Supporting Information, Figure S2e). The result confirmed that the as-prepared Ag NCs were protected by GSH on the surface. The spectroscopic features of the aqueous Ag-GSH NCs are shown in Figure 1.

As indicated in Figure 1a, the absorption band of the Ag-GSH NCs gave a peak at 490 nm, which was associated with the presence of four to nine silver atoms in the Ag NCs.[19] In addition, the absorption spectra did not show the charac-
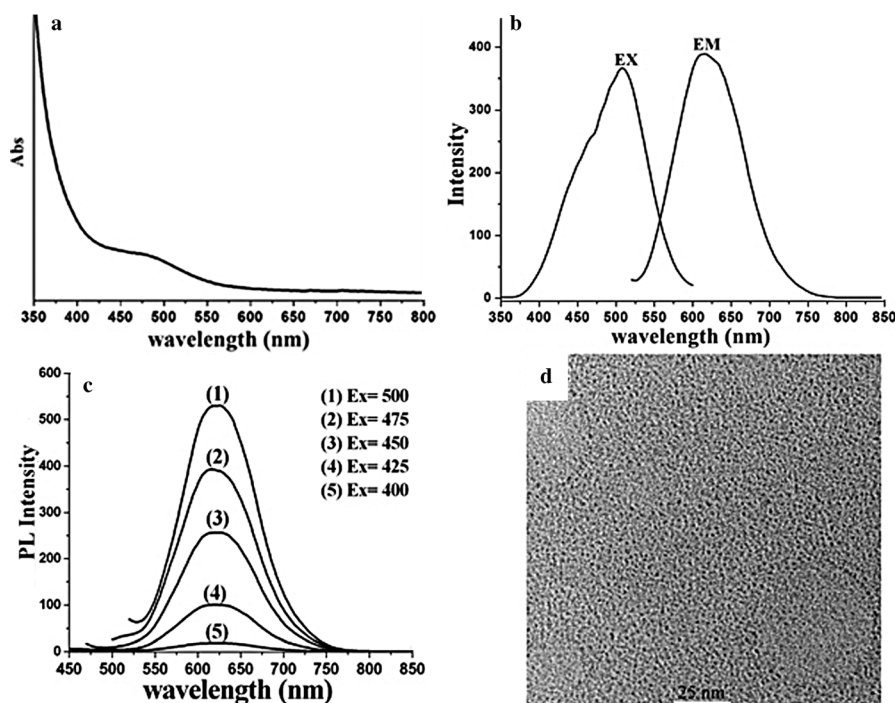

Figure 1. a) UV/Vis spectrum and b) excitation (EX) and emission (EM) spectra of resultant fluorescent GSH-Ag NCs in aqueous solution; c) resultant photoluminescence (PL) intensity of fluorescent GSH-Ag NCs in aqueous solution excited at different wavelengths: 1) 500, 2) 475, 3) 450, 4) 425, 5) 400; d) TEM image of resultant fluorescent GSH-Ag NCs.

teristic plasmon absorption of Ag nanoparticles, which strongly suggested the formation of complexes between Ag NCs and GSH.[20] The photoluminescence (PL) emission and excitation spectra was shown in Figure 1b. In aqueous solution, the Ag-GSH NCs exhibited red fluorescence with $\lambda_{max}=620$ nm; the full width at half maximum was around 100 nm. Unlike semiconductor quantum dots, these newly developed Ag-GSH NCs gave a well-defined excitation band with $\lambda_{max}=508$ nm. To confirm that the luminescence came from the Ag NCs instead of random light scatting, irradiation was conducted at different wavelengths (Figure 1c). With excitation wavelength between 400 and 500 nm, the PL intensity varied, with the maximum PL observed using irradiation at 500 nm. The shape and the emission wavelength did not change with various excitation lights, which confirmed that the red fluorescence emission was due to the Ag NCs. To ensure the optimal reaction time for the synthesis of this GSH-Ag NCs, time-dependent UV/Vis and PL measurements were conducted (see the Supporting Information, Figure S3). The spectra clearly revealed that upon the treatment with hydrazine reductants, the PL intensity of the reaction mixture increased and reached a maximum at 11 h. Extension of the reaction time caused the rapid decrease of the fluorescence intensity, which suggested decomposition or aggregation of the Ag-GSH NCs for extended treatment with the reductants.

The transmission electron microscopy (TEM) image of the Ag-GSH NCs is shown in Figure 1d. As indicated, this preparation method gave NCs with an average size below 2.0 nm (see the Supporting Information, Figure S4). Moreover, there was no formation of larger Ag nanoparticles or aggregates, which highlighted the unique template effect by glutathione for the preparation of small Ag NCs. Figure S5 in the Supporting Information shows the TEM image for a larger view. The X-ray powder diffraction (XRD) pattern showed a broad diffraction peak at $2\theta = 20-40°$ (see the Supporting Information, Figure S6). The Ag nanoparticles showed no crystalline structure, as the NCs were too small to express all diffraction peaks typical of bulk Ag nanoparticles; a similar result was also observed for Au25 NCs.[21]

The time-dependent spectra (see the Supporting Information, Figure S3) indicated that there was no fluorescence emission before the addition of the hydrazine reductant. The red emission at $\lambda_{max}=620$ nm appeared 30 minutes after the addition of $NH_2NH_2 \cdot 2H_2O$, and the fluorescence intensity reach the maximum after 11 h at room temperature. No noticeable red shift or blue shift was observed during the process, and the full width at half maximum was around 100 nm, which indicated the narrow size distribution of the formed Ag NCs. Further increase of the reaction time caused the rapid decrease of the PL intensity, and almost no emission was observed after treating the reaction mixture for 53 h. These results not only helped the development of optimal preparation protocols as reported in Scheme 1 but also further confirmed that the observed PL emission was directly attributed to the formation of the Ag NCs, as proposed.

With these fluorescent, water-soluble Ag NCs in hands, we then investigated their ability as sensors for the selective detection of metal cations. Our general hypothesis was that the free COOH and NH_2 groups on GSH could provide binding handles to bring metal cations close to the Ag NCs. As a result, the fluorescence of Ag NCs would be quenched, which could lead to the desired metal cation sensing. The key concerns for this design were: 1) how effective the quenching will be; 2) will this very simple surface modification (by GSH) give good selectivity, and; 3) will the fluorescence quenching possess a linear relationship with cation's concentration, which is crucial for any quantitative determination. A series of metal cation solutions were then employed to interact with this new type of fluorescence sensor (Figure 2a).
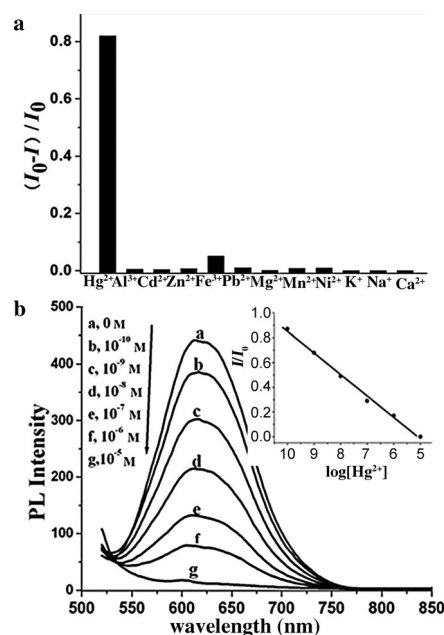

Figure 2. a) The PL intensity quenching of fluorescent GSH-Ag NCs at 620 nm in the presence of 10^{-6} M metal ions. b) The PL emission spectra of fluorescent GSH-Ag NCs in the presence of Hg^{2+} with various concentrations; the inset shows the relative luminescent intensity (I/I_0) versus various concentrations of Hg^{2+}.

To our great surprise and pleasure, under identical concentration (10^{-6} M) and parallel testing conditions, the Ag NCs showed excellent selectivity toward Hg^{2+} over other tested metal cations, including Cd^{2+}, Pb^{2+}, Al^{3+}, and Zn^{2+}. Moreover, a linear relationship (inset, Figure 2b) was observed between the Ag NCs fluorescence intensity and the logarithm of the concentration of Hg^{2+} ions over the range from 0.1 nM to 10 μM (based on the fluorescence spectra in Figure 2b). A similar linear relationship was also observed for metal ions (Hg^{2+} and Cu^{2+}) detection by fluorescent Au nanodots stabilized by 11-mercaptoundecanol and bovine serum albumin (BSA).[9b,22] The Ag NCs indicated extremely high sensitivity with limit of detection (LOD) as low as 10^{-10} M (0.02 ppb, 0.1 nM). There was no emission wavelength shift with all different concentrations. In addition to Hg-

$(NO_3)_2$, $Hg(OAc)_2$ as another Hg^{2+} salt was investigated. The same result as with $Hg(NO_3)_2$ was obtained. The Ag NCs indicated extremely high sensitivity with a limit of detection (LOD) as low as 10^{-10} M (0.02 ppb, 0.1 nM). There was no emission wavelength shift with different concentrations (see the Supporting Information, Figure S7a). A linear relationship was observed between the Ag NCs fluorescence intensity and the logarithm of the concentration of Hg^{2+} ions over the range from 0.1 nM to 10 μM (based on the fluorescence spectra of Figure S7b).

The fluorescence of NCs depends not only on the metal quantization effect but also on the surface ligands or scaffolds.[23] Herein, the surface of the Ag NCs was protected by GSH, which was confirmed by FTIR spectroscopy and XPS analysis. This was important for making them highly selective and sensitive for Hg^{2+} detection, owing to free functional groups, such as free carboxy, in GSH. The highly sensitive and selective fluorescence sensor activity for Hg^{2+} is based on the aggregation-induced fluorescence quenching of glutathione-capped fluorescent Ag NCs.[24] The carboxylic acids on the surface of Ag NCs have a much stronger affinity toward Hg^{2+} ($\log \beta_4 = 17.6$).[25] The free carboxylic acids could easily interact with Hg^{2+} and form large aggregates of nanoparticles by an ion-templated chelation process.[26] The aggregation of Ag NCs induced by Hg^{2+} was confirmed by TEM (Figure S8 in the Supporting Information). We found that the Hg^{2+}-induced aggregation of the as-prepared fluorescent Ag-GSH NCs reached completion and left only lager aggregates (Figure S8 in the Supporting Information), which caused the luminescence quenching of Ag NCs. This sensing mechanism based on aggregation-induced fluorescence quenching has been widely adopted for NCs as sensor probes to detect metal ions.[3d,9b,27]

It is well known that highly sensitive and selective detection of Hg^{2+} in water is crucial for environmental and biological applications. One critical challenge was to have a practical Hg^{2+} sensor with high sensitivity. While the current testing standard for the United States Environmental Protection Agency (EPA) is 2 ppb (10 nM) and for the European Union is 1 ppb (5 nM), the reported GSH-Ag NCs sensor has lower detecting limit than both standards.[28] To our knowledge, this system provided the highest Hg^{2+} detection sensitivity among all sensors reported to date, especially those based on fluorescent Ag NCs.[3d,10,29] Figure 3 shows the control assays, which indicated that competing cations, such as Na^+, K^+, Ca^{2+}, and Mg^{2+}, did not influence the Hg^{2+} quenching effectiveness, even with 10^7 higher cation concentration. In order to determine the real application for Hg^{2+} detection, the Hg^{2+} analysis in drinking water solution was investigated. As shown in Figure 4, although the fluorescence was affected in drinking water due to the complex environment including the various cations and pH value, the fluorescence of as-prepared Ag NCs was quenched with increasing the Hg^{2+} concentration, and the detection for Hg^{2+} was also highly sensitive, at approximately 1 nM (0.2 ppb), which suggested that the as-prepared Ag NCs as Hg^{2+} detection probe have the potential for real application.
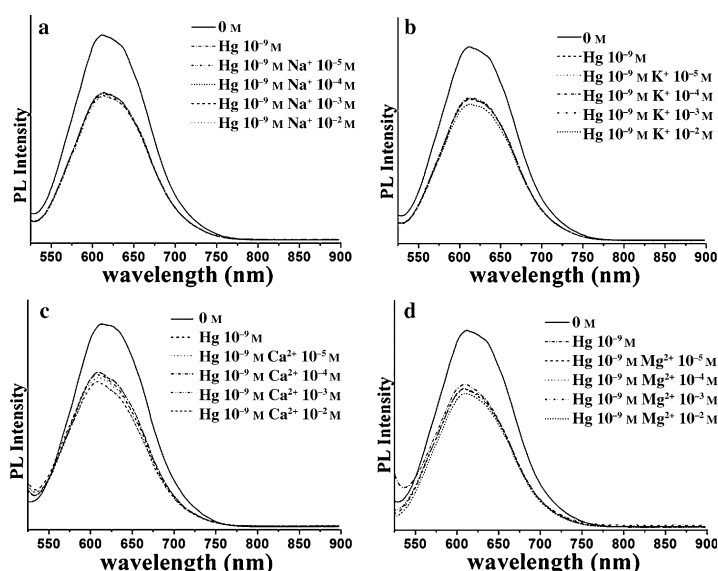

Figure 3. Hg^{2+} detection with competing cations a) Na^+; b) K^+; c) Ca^{2+}; d) Mg^{2+}.
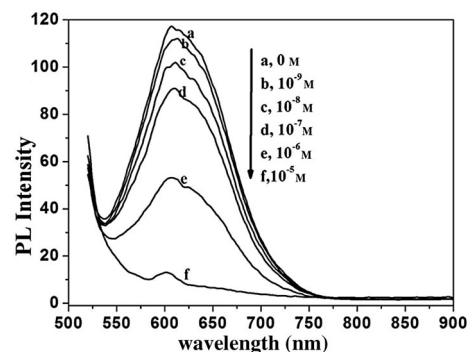

Figure 4. The highly sensitive detection of Hg^{2+} in drinking water; the limit of detection (LOD) was as low as approximately 1 nM (0.2 ppb).

Conclusions

In conclusion, a practical and robust synthesis of water-soluble and fluorescent small Ag NCs was successfully developed through the application of GSH as the template. This newly developed Ag NCs indicated excellent selectivity and sensitivity for Hg^{2+} detection in water. Although the exact mechanism regarding the resulting exceptional sensor performance is subject to further investigation, the reported system demonstrates a new approach for sensor development using fluorescent Ag NCs with a small peptide as a potential handle for substrate recognition, and further evolution of this strategy is certainly expected to be applied in related fields.

Experimental Section

Experimental details can be found in the Supporting Information.

FULL PAPERS

Preparation of GSH-stabilized Ag NCs

In a typical experiment, the aqueous solution of GSH (50 mM, 5 mL) was added to the aqueous solution of $AgNO_3$ (50 mM, 5 mL). The transparent solution changed to a white supramolecular hydrogel when the pH value of solution was 1.88. Then 1 M NaOH solution was added dropwise until the pH value of solution was 6.45 and the solution became colorless and transparent. Then, $N_2H_4 \cdot 2H_2O$ (1 mL, 85 wt%) aqueous solution as the reducing agent was injected, and the pH value rose to 10.18. The color of the reaction solution changed from colorless to yellow over about 11 h at room temperature. The resultant GSH-Ag nanocluster complexes were precipitated by addition of isopropyl alcohol, collected through centrifugal at 8000 r min^{-1}, and then redispersed in water. The purification process was repeated three times at room temperature, and the nanoclusters were dispersed in water (10 mL) for further application.

Application as Hg^{2+} sensor

Mercury(II) nitrate was used for the study of Hg^{2+} detection. Solutions with various Hg^{2+} concentrations from 10^{-5} M to 10^{-10} M were prepared. For the sensor study, aqueous solution of as-prepared GSH-Ag nanocluster complexes (0.5 mL) and Hg^{2+} solution (2.5 mL) with different concentrations were mixed and allowed to equilibrate for 1 min before the spectral measurements. To check the cation selectivity of this sensor, we also tested other metal ions, including K^+, Na^+, Ca^{2+}, Zn^{2+}, Mg^{2+}, Pb^{2+}, Ni^{2+}, Al^{3+}, Cd^{2+}, Mn^{2+}, and Fe^{3+} using the same procedure that was used for the detection of Hg^{2+}.

Acknowledgements

[1] a) W. T. Wei, Y. Z. Lu, W. Chen, S. W. Chen, *J. Am. Chem. Soc.* **2011**, *133*, 2060–2063; b) S. I. Tanaka, J. Miyazaki, D. K. Tiwari, T. Jin, Y. Inouye, *Angew. Chem.* **2011**, *123*, 451–455; *Angew. Chem. Int. Ed.* **2011**, *50*, 431–435; c) B. S. González, M. J. Rodríguez, C. Blanco, J. Rivas, M. A. López-Quintela, J. M. G. Martinho, *Nano Lett.* **2010**, *10*, 4217–4221; d) L. Shang, S. J. Dong, *Chem. Commun.* **2008**, 1088–1090.

[2] a) H. Xu, K. S. Suslick, *Adv. Mater.* **2010**, *22*, 1078–1082; b) I. Díez, R. H. A. Ras, *Nanoscale* **2011**, *3*, 1963–1970.

[3] a) E. G. Gwinn, P. O'Neill, A. J. Guerrero, D. Bouwmeester, D. K. Fygenson, *Adv. Mater.* **2008**, *20*, 279–283; b) W. Guo, J. Yuan, Q. E. Dong, E. Wang, *J. Am. Chem. Soc.* **2010**, *132*, 932–934; c) J. Zheng, R. M. Dickson, *J. Am. Chem. Soc.* **2002**, *124*, 13982–13983; d) C. Guo, J. Irudayaraj, *Anal. Chem.* **2011**, *83*, 2883–2889; e) I. Richards, S. Choi, J. C. Hsiang, Y. Antoku, T. Vosch, A. Bongiorno, Y. L. Tzeng, R. M. Dickson, *J. Am. Chem. Soc.* **2008**, *130*, 5038–5039; f) Z. Shen, H. Duan, H. Frey, *Adv. Mater.* **2007**, *19*, 349–352.

[4] a) Y. Bao, H. Yeh, C. Zhong, S. A. Ivanov, J. K. Sharma, M. L. Neidig, D. M. Vu, A. P. Shreve, R. B. Dyer, J. H. Werner, J. S. Martinez, *J. Phys. Chem. C* **2010**, *114*, 15879–15882; b) B. Adhikari, A. Banerjee, *Chem. Mater.* **2010**, *22*, 4364–4371.

[5] a) A. D. Stevens, M. C. Symons, *J. Chem. Soc. Faraday Trans. 1* **1989**, *85*, 1439; b) A. Henglein, *Chem. Phys. Lett.* **1989**, *154*, 473;

c) M. Choi, Z. J. Wu, E. Iglesia, *J. Am. Chem. Soc.* **2010**, *132*, 9129–9137; d) G. D. Cremer, E. Coutiño-Gonzalez, M. B. J. Roeffaers, B. Moens, J. Ollevier, M. V. Auweraer, R. Schoonheydt, P. A. Jacobs, F. C. D. Schryver, J. Hofkens, D. E. D. Vos, B. F. Sels, T. Vosch, *J. Am. Chem. Soc.* **2009**, *131*, 3049–3056.

[6] E. M. Nolan, S. J. Lippard, *Chem. Rev.* **2008**, *108*, 3443.

[7] a) M. Valko, H. Morris, M. T. D. Cronin, *Curr. Med. Chem.* **2005**, *12*, 1161–1208; b) Y. Q. Chen, H. Bai, W. J. Hong, G. Q. Shi, *Analyst* **2009**, *134*, 2081–2086.

[8] a) S. Wang, E. S. Forzani, N. Tao, *Anal. Chem.* **2007**, *79*, 4427–4432; b) Y. K. Yang, K. J. Yook, J. Tae, *J. Am. Chem. Soc.* **2005**, *127*, 16760–16761; c) P. Chen, C. He, *J. Am. Chem. Soc.* **2004**, *126*, 728–729; d) I. B. Kim, U. H. F. Bunz, *J. Am. Chem. Soc.* **2006**, *128*, 2818–2819.

[9] a) J. P. Xie, Y. G. Zheng, J. Ying, *Chem. Commun.* **2010**, *46*, 961–963; b) C. C. Huang, Z. Yang, K. H. Lee, H. T. Chang, *Angew. Chem.* **2007**, *119*, 6948–6952; *Angew. Chem. Int. Ed.* **2007**, *46*, 6824–6828.

[10] W. Guo, J. Yuan, E. Wang, *Chem. Commun.* **2009**, 3395–3397.

[11] N. Cathcart, P. Mistry, C. Makra, B. Pietrobon, N. Coombs, M. Jelokhani-Niaraki, V. Kitaev, *Langmuir* **2009**, *25*, 5840.

[12] a) S. Kumar, M. D. Bolan, T. P. Bigioni, *J. Am. Chem. Soc.* **2010**, *132*, 13141; b) B. Baruwati, V. Polshettiwar, R. S. Varma, *Green Chem.* **2009**, *11*, 926.

[13] I. Odriozola, I. Loinaz, J. A. Pomposo, H. J. Grande, *J. Mater. Chem.* **2007**, *17*, 4843–4845.

[14] M. X. Yu, C. Zhou, J. B. Liu, J. D. Hankins, J. Zheng, *J. Am. Chem. Soc.* **2011**, *133*, 11014–11017.

[15] J. S. Shen, D. H. Li, Q. G. Cai, Y. B. Jiang, *J. Mater. Chem.* **2009**, *19*, 6219–6224.

[16] T. U. B. Rao, B. Nataraju, T. Pradeep, *J. Am. Chem. Soc.* **2010**, *132*, 16304–16307.

[17] E. S. Shibu, T. Pradeep, *Chem. Mater.* **2011**, *23*, 989–999.

[18] F. Xia, L. Feng, S. T. Wang, T. L. Sun, W. L. Song, W. H. Jiang, L. Jiang, *Adv. Mater.* **2006**, *18*, 432–436.

[19] J. Zhang, S. Xu, E. Kumacheva, *Adv. Mater.* **2005**, *17*, 2336–2340.

[20] D. G. Shchukin, I. L. Radtchenko, G. B. Sukhorukov, *ChemPhysChem* **2003**, *4*, 1101–1103.

[21] M. A. H. Muhammed, T. Pradeep, *Small* **2011**, *7*, 204–208.

[22] H. Y. Liu, X. Zhang, X. M. Wu, L. P. Jiang, C. Burda, J. J. Zhu, *Chem. Commun.* **2011**, *47*, 4237–4239.

[23] F. Wen, Y. H. Dong, L. Feng, S. Wang, S. C. Zhang, X. R. Zhang, *Anal. Chem.* **2011**, *83*, 1193–1196.

[24] Y. M. Guo, Z. Wang, H. W. Shao, X. Y. Jiang, *Analyst* **2012**, *137*, 301–304.

[25] R. K. Bera, A. K. Das, C. R. Raj, *Chem. Mater.* **2010**, *22*, 4505–4511.

[26] C.-C. Huang, H.-T. Chang, *Chem. Commun.* **2007**, 1215–1217.

[27] a) W. B. Chen, X. J. Tu, X. Q. Guo, *Chem. Commun.* **2009**, 1736–1738; b) N. Goswami, A. Giri, M. S. Bootharaju, P. L. Xavier, T. Pradeep, S. K. Pal, *Anal. Chem.* **2011**, *83*, 9676–9680.

[28] *Dynamics of Mercury Pollution on Regional and Global Scales: Atmospheric Processes and Human Exposures Around the World* (Eds.: N. Pirrone, K. R. Mahaffey), Springer, **2005**, New York.

[29] a) H. Wei, Z. D. Wang, L. M. Yang, S. L. Tian, C. J. Hou, Y. Lu, *Analyst* **2010**, *135*, 1406–1410; b) M. Li, Q. Y. Wang, X. D. Shi, L. A. Hornak, N. Q. Wu, *Anal. Chem.* **2011**, *83*, 7061–7065.